

The TCR's sensitivity to self peptide–MHC dictates the ability of naive CD8⁺ T cells to respond to foreign antigens

Ross B Fulton¹, Sara E Hamilton¹, Yan Xing¹, J Adam Best², Ananda W Goldrath², Kristin A Hogquist¹ & Stephen C Jameson¹

The strength with which complexes of self peptide and major histocompatibility complex (MHC) proteins are recognized by the T cell antigen receptor (TCR) dictates the homeostasis of naive CD8⁺ T cells, but its effect on reactivity to foreign antigens is controversial. As expression of the negative regulator CD5 correlates with self-recognition, we studied CD5^{lo} and CD5^{hi} naive CD8⁺ T cells. Gene-expression characteristics suggested CD5^{hi} cells were better poised for reactivity and differentiation than were CD5^{lo} cells, and we found that the CD5^{hi} pool also exhibited more efficient clonal recruitment and expansion, as well as enhanced reactivity to inflammatory cues, during the recognition of foreign antigen. However, the recognition of complexes of foreign peptide and MHC was similar for both subsets. Thus, CD8⁺ T cells with higher self-reactivity dominate the immune response to foreign antigens, with implications for T cell repertoire diversity and autoimmunity.

The nature of the interaction of the T cell antigen receptor (TCR) with complexes of foreign peptide and major histocompatibility complex (MHC) proteins (foreign peptide–MHC) determines the magnitude of the response and differentiation characteristics of antigen-specific T cells^{1–4}. In addition, studies suggest that interactions of the TCR with self peptide–MHC also affect the response of naive T cells to foreign peptide–MHC^{5–11}. Thymic positive selection and naive T cell homeostasis require low-affinity recognition of self peptide–MHC by the TCR^{12–16}, but there is controversy about how such interactions affect the subsequent response to foreign peptide–MHC: published studies indicate that the recognition of self peptide–MHC enhances⁶ or diminishes⁷ the response to foreign antigens or selectively impairs sensitivity to low-affinity foreign ligands¹⁴. However, those reports investigated the effect of withdrawal of self peptide–MHC rather than studying how the degree of sensitivity to self peptide–MHC influences the T cell response to foreign peptide–MHC.

Homeostatic interactions of the TCR with self peptide–MHC are thought to be of very low affinity and to involve the recognition of multiple self peptides by an individual T cell clone, which would preclude direct assessment of the characteristics of self peptide–MHC recognition in the polyclonal T cell pool. However, differences in expression of the cell surface protein CD5 have proven to be a valuable surrogate for the strength of TCR–self peptide–MHC interactions^{14,17–21}. CD5 expression on naive T cells can be used to accurately predict basal TCR signaling intensity and the ability of T cells to rapidly engage key TCR signaling pathways^{9–11}, and it correlates with the ability of naive CD8⁺ T cells to respond to homeostatic cues^{22–26}.

However, the underlying basis for the distinct response characteristics of naive CD5^{lo} and CD5^{hi} populations is unclear, as is the effect of these differences on reactivity to foreign peptide–MHC.

Published studies have used CD5 expression on naive CD4⁺ T cells to correlate the strength of self peptide–MHC interactions with reactivity to foreign peptide–MHC^{9–11}. In one study, analysis of mice with transgenic expression of the TCR suggested a direct correlation between the abundance of CD5 on the cell surface and the ability of the cell to bind tetramers of cognate foreign peptide–MHC⁹, which suggested that the affinity of the TCR for self peptide–MHC can be used to predict its affinity for foreign peptide–MHC. Those authors observed more vigorous responses by CD5^{hi} naive CD4⁺ T cells than by their CD5^{lo} counterparts to foreign peptide–MHC. Another report failed to observe any correlation between CD5 expression and affinity of the TCR for foreign peptide–MHC ligands, however, and found that CD5^{lo} T cell populations expanded more efficiently than their CD5^{hi} counterparts during the primary response to foreign antigen^{10,11}. Hence, whether and how CD5 expression can be used to predict the capacity with which naive T cells bind to and/or respond toward foreign peptide–MHC ligands is unclear.

Here we report that CD5^{hi} and CD5^{lo} naive CD8⁺ T cells differed in gene-expression characteristics and that the CD5^{hi} population manifested improved clonal recruitment and expansion in response to foreign peptide–MHC. These differences in response did not correlate with the strength of the interaction of the TCR with foreign peptide–MHC, but CD5^{hi} naive CD8⁺ T cells showed superior use of *in vivo* inflammatory signals. Our data suggest that predetermined heterogeneity

¹Department of Laboratory Medicine and Pathology, Center for Immunology, University of Minnesota Medical School, Minneapolis, Minnesota, USA. ²Division of Biological Sciences, University of California San Diego, La Jolla, California, USA. Correspondence should be addressed to S.C.J. (james024@umn.edu).

Received 1 April; accepted 27 October; published online 24 November 2014; doi:10.1038/ni.3043

among naive T cells dictates the capacity of their response to foreign antigens, with consequences for diversity of the functional T cell repertoire. Moreover, the finding that T cells with strong reactivity to self peptide–MHC dominated the response to foreign peptide–MHC has implications for the outgrowth of autoreactive T cells.

RESULTS

Distinct phenotypes of CD5^{hi} versus CD5^{lo} CD8⁺ T cells

We first assessed phenotypic differences between CD5^{lo} naive (CD44^{lo}CD122^{lo}) CD8⁺ T cells and their CD5^{hi} counterparts. In an extension of published work^{24,26,27}, we found that the CD5^{hi} cells were slightly larger, had higher expression of the adhesion molecule CD44 and modestly higher expression of the cytokine receptors IL-2R β (CD122) and IL-7R α (CD127), but slightly lower expression

of the TCR, coreceptor CD8 and adhesion molecule CD62L, than the CD5^{lo} cells had (Fig. 1a and Supplementary Fig. 1a–c). The CD5^{hi} naive CD8⁺ T cell population also showed elevated expression of T-bet and eomesodermin (transcription factors associated with the differentiation of activated CD8⁺ T cells²⁸), and a subset of CD5^{hi} cells expressed the chemokine receptor CXCR3 (Fig. 1a). The phenotypic characteristics of CD5^{hi} naive CD8⁺ T cells had some similarities to those of memory CD8⁺ T cells. However, the frequency and phenotype of CD5^{hi} naive CD8⁺ T cells was similar in wild-type mice and mice deficient in interleukin 15 (IL-15), which lack typical CD8⁺ memory T cells²⁹ (Fig. 1b and Supplementary Fig. 1b,c). Hence, the CD5^{hi} naive CD8⁺ T cell population neither derived from nor depended on memory-phenotype CD8⁺ T cells.

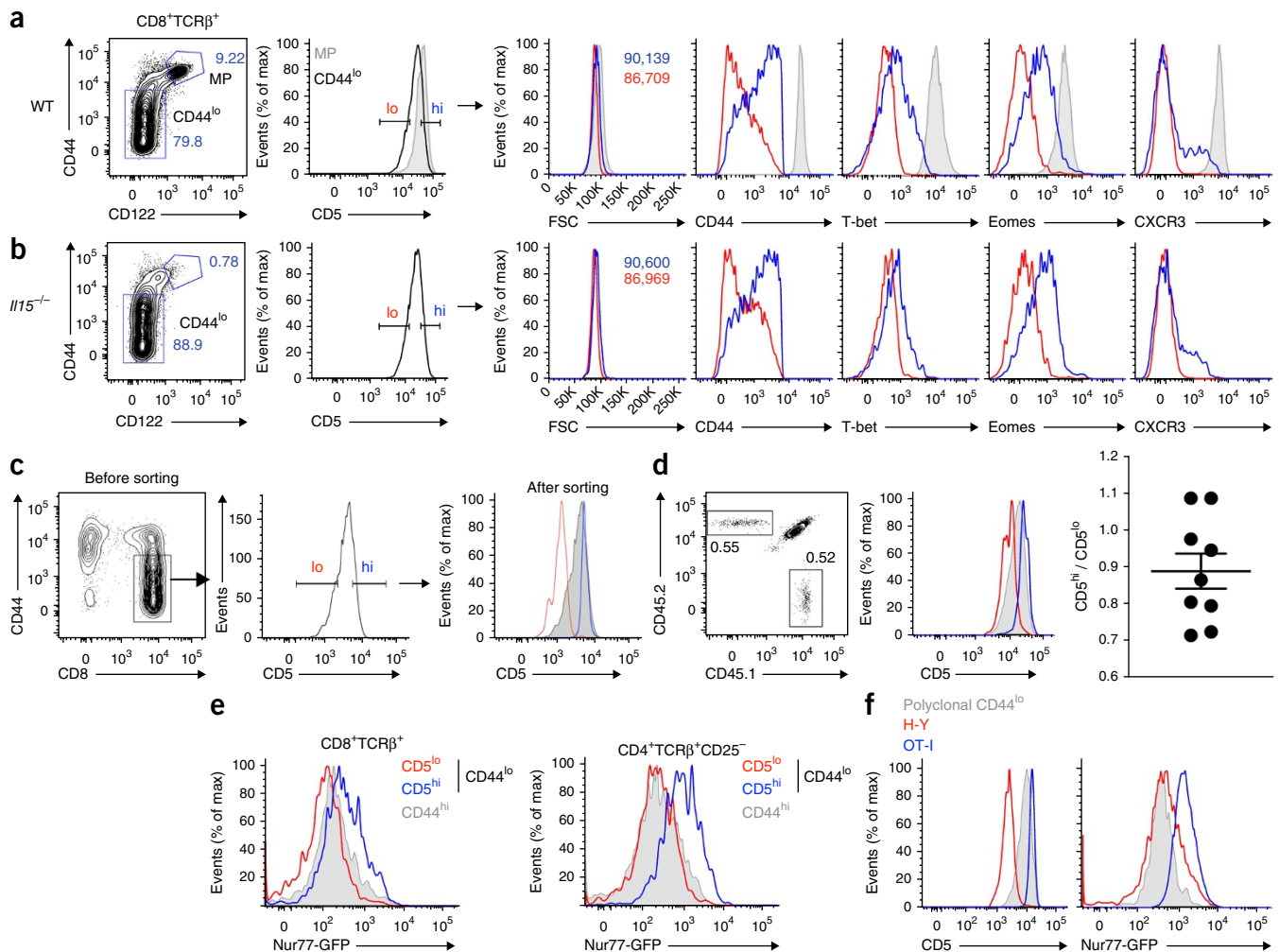


Figure 1 CD5 expression by naive CD8⁺ T cells identifies stable populations with unique phenotypic traits. **(a,b)** Flow cytometry of cells pooled from the spleen and lymph nodes of wild-type mice **(a)** or *Il15*^{-/-} mice **(b)**, stained for CD44, T-bet, Eomes and CXCR3 (right), gated on naive (CD44^{lo}CD122^{lo}) CD8⁺ T cells with the lowest 20% (lo) and highest 20% (hi) CD5 expression (gating at left). Gray shaded curves (right), cells with memory phenotype (CD44^{hi}CD122^{hi}). FSC, forward scatter (a measure of cell size). Numbers adjacent to outlined areas (far left, **d**) indicate percent CD45.2^{hi}CD45.1^{lo} cells (bottom left) or CD45.2^{lo}CD45.1^{hi} cells (top right). **(e)** Flow cytometry of CD4⁺CD25⁻ and CD8⁺ T cells from *Nur77*^{GFP} mice, gated on CD5 expression (as in **a,b**), followed by analysis of Nur77-GFP expression (gray curves as in **a,b**). **(f)** Flow cytometry of H-Y or OT-I CD8⁺ T cells and of polyclonal naive CD8⁺ T cells (gray), gated on the CD44^{lo} population, assessing expression CD5 and Nur77-GFP. Data are representative of four **(a,c,d)**, two **(b,f)** or three to four **(e)** independent experiments ($n = 10$ mice **(a)**, 9 mice **(c,d)**, 4 mice **(b)**, 6–7 mice **(f)** or 6–11 mice **(e)**).

To determine whether the CD5^{hi} and CD5^{lo} populations were stable, we sorted polyclonal naive CD8⁺ T cells into CD5^{hi} or CD5^{lo} populations (which reflected the upper and lower 20% of distribution of CD5 expression, respectively) and transferred congenically distinct cell populations together into normal recipients. Both transferred populations maintained distinct CD5 expression and persisted for at least 8 weeks (Fig. 1c,d and data not shown), indicative of equivalent steady-state survival (similar to results obtained in studies of naive CD4⁺ T cells⁹). The majority of donor cells maintained a naive phenotype, although a fraction of the CD5^{hi} cells converted to a CD44^{hi} phenotype (Supplementary Fig. 1d), consistent with their enhanced response to homeostatic cues^{22–26}.

Biochemical approaches indicate a correlation between CD5 abundance and the degree of basal TCR signaling^{5,9,11}; however, such methods do not permit assessment of TCR signal strength in individual cells. Hence, we studied *Nur77*^{GFP} transgenic reporter mice, in which expression of green fluorescent protein (GFP) from the immediate-early gene encoding the nuclear hormone receptor *Nur77* (*Nr4a1*; called ‘*Nur77*’ here) provides a sensitive ‘readout’ of TCR signaling³⁰. In CD8⁺ and CD4⁺ naive T cell subsets, CD5^{hi} cells showed higher GFP expression than that of the CD5^{lo} population (Fig. 1e), and this correlation held for *Nur77*^{GFP} expression in CD8⁺ T cells from H-Y mice (which have transgenic expression of a male antigen-specific MHC class I-restricted TCR) and OT-I mice (which have transgenic expression of an ovalbumin-specific, MHC class I-restricted TCR), which reflect CD5^{lo} populations and CD5^{hi} populations, respectively^{9,22,25} (Fig. 1f). Thus, CD5^{hi} naive CD8⁺ T cells and their CD5^{lo} counterparts were distinct, stable populations, with CD5^{hi} cells displaying characteristics of cells that undergo more intense or frequent interactions of the TCR with self peptide–MHC.

Transcriptional profiles of CD5^{hi} versus CD5^{lo} CD8⁺ T cells

We next conducted gene-expression analysis of polyclonal CD5^{hi} and CD5^{lo} naive CD8⁺ T cells. In total, 57 genes showed a significant difference in expression of at least twofold in CD5^{hi} naive CD8⁺ T cells relative to their expression in CD5^{lo} naive CD8⁺ T cells (47 were upregulated and 10 were downregulated; Table 1). Among genes upregulated in CD5^{hi} cells were those encoding the transcription factors *Eomes*, *T-bet*, *Helios* and *Id3*, many of which have key roles in the differentiation of activated T cells²⁸, and molecules associated with the trafficking and adhesion of effector T cells (*CXCR3*, *XCL1* and *CD44*). Conversely, the gene encoding the kinase *Itk* (which can serve as a negative regulator of *T-bet*^{31,32}) was downregulated in CD5^{hi} cells.

We further investigated the expression of *XCL1*, since it has been associated with efficient *in vivo* activation of CD8⁺ T cells (via enhancing the colocalization of T cells and dendritic cells (DCs))³³. After brief *in vitro* stimulation of splenocytes, expression of *XCL1* protein was biased to a subpopulation of CD5^{hi} naive CD8⁺ T cells (Fig. 2a,b and Supplementary Fig. 2a). Expression of *CXCR3* and *T-bet* also marked a subset of CD5^{hi} naive CD8⁺ T cells (Fig. 2b and Supplementary Fig. 2a). However, although memory-phenotype (CD44^{hi}) CD8⁺ T cells typically coexpressed these proteins, there was little coordinated expression of these in the naive CD5^{hi} pool (Supplementary Fig. 2b,c), which indicated considerable heterogeneity within the CD5^{hi} naive CD8⁺ T cell population.

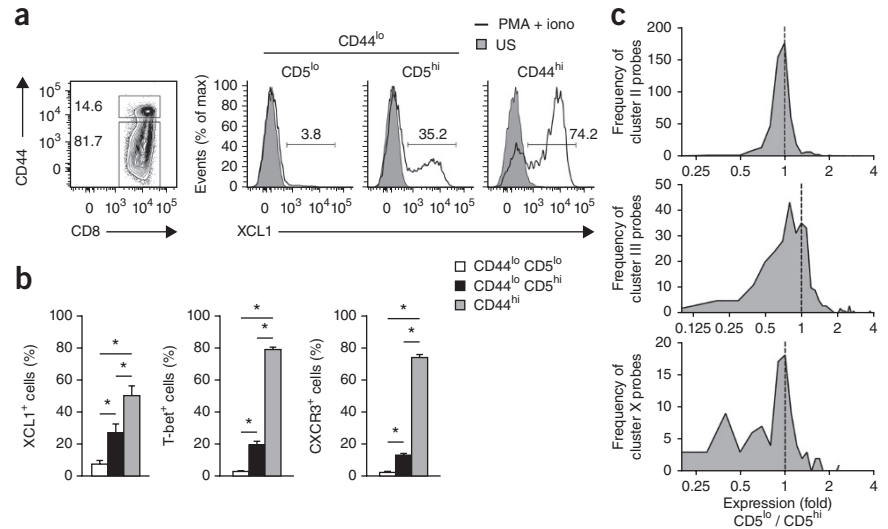
Most differences between the CD5^{hi} and CD5^{lo} naive CD8⁺ T cell populations in their expression of individual genes were subtle (Table 1); hence, we explored whether there was enrichment in the expression of specific gene clusters. For a focused comparison, we used a χ^2 test to

Table 1 Gene expression in sorted CD5^{hi} and CD5^{lo} naive polyclonal CD8⁺ T cells

Up	Gene	Expression (fold)	P
1	A430093F15Rik	7.16	0.0170
2	<i>Endod1</i>	5.79	0.0233
3	<i>Cxcr3</i>	5.60	0.0217
4	A530021J07Rik	5.48	0.0033
5	<i>Ly6C1</i>	5.27	0.0200
6	<i>Tbx21</i> (T-bet)	4.96	0.0019
	A530021J07Rik	4.74	0.0113
	A530021J07Rik	3.66	0.0144
7	<i>Ndr1</i>	3.42	0.0224
8	<i>Eomes</i>	3.41	0.0255
9	<i>Ighv14-2</i>	3.28	0.0059
10	<i>Cobll1</i>	3.11	0.0033
11	<i>Ms4a4c</i>	3.08	0.0172
12	<i>Reck</i>	3.02	0.0201
13	<i>Itih5</i>	3.00	0.0391
14	<i>Phactr2</i>	2.97	0.0431
15	<i>Bcat1</i>	2.91	0.0122
16	<i>Cldn10</i>	2.88	0.0039
17	9230110F15Rik	2.85	0.0293
18	<i>Serf1</i>	2.76	0.0314
19	<i>Ptgfrn</i>	2.72	0.0458
20	<i>Xcl1</i>	2.70	0.0173
	<i>Eomes</i>	2.65	0.0361
21	<i>Plac8</i>	2.60	0.0137
22	<i>Rrm2</i>	2.58	0.0286
23	<i>Fahd1</i>	2.52	0.0457
24	<i>Mcart6</i>	2.43	0.0019
	<i>Ms4a4c</i>	2.41	0.0179
25	<i>Ikzf2</i> (Helios)	2.40	0.0273
26	<i>Xdh</i>	2.40	0.0031
27	BB557941	2.40	0.0484
28	<i>Cd200</i>	2.27	0.0288
29	<i>Anxa2</i>	2.26	0.0213
	<i>Ndr1</i>	2.23	0.0047
30	<i>Gsto1</i>	2.21	0.0197
31	<i>Cd5</i>	2.20	0.0034
32	<i>Ptpn4</i>	2.20	0.0291
33	<i>Chst11</i>	2.17	0.0097
34	<i>Armcx4</i>	2.15	0.0115
35	<i>Top2a</i>	2.15	0.0321
36	<i>Hopx</i>	2.14	0.0143
	<i>Ndr1</i>	2.12	0.0008
37	<i>Il10</i>	2.10	0.0249
38	<i>Stmn1</i>	2.09	0.0357
39	<i>Mrpl35</i>	2.09	0.0337
40	<i>Lilrb3</i> , <i>Pira1</i> , <i>Pira2</i>	2.08	0.0021
41	<i>Coro2a</i>	2.07	0.0034
42	<i>Cd44</i>	2.06	0.0072
43	<i>Kctd15</i>	2.03	0.0268
44	<i>Pogk</i>	2.03	0.0124
45	<i>Id3</i>	2.02	0.0049
46	<i>Pck1</i>	2.02	0.0151
47	<i>Aim1</i>	2.02	0.0227
Down	Gene	Expression (fold)	P
1	<i>Dntt</i>	9.27	0.0110
2	<i>Slc6a19</i>	4.18	0.0025
	<i>Slc6a19</i>	4.10	0.0143
3	<i>Slc16a5</i>	2.79	0.0257
4	<i>Ddc</i>	2.55	0.0035
5	A130038J17Rik	2.30	0.0175
6	<i>Grik4</i>	2.20	0.0034
7	<i>Tmem154</i>	2.10	0.0322
8	4930513N10Rik	2.08	0.0453
9	<i>Tubb2a</i>	2.03	0.0200
10	<i>Itk</i>	2.01	0.0411

Expression of 47 genes upregulated (Up) and 10 genes downregulated (Down) in sorted CD5^{hi} naive polyclonal CD8⁺ T cells relative to their expression in CD5^{lo} naive polyclonal CD8⁺ T cells, among those with a significant ($P < 0.05$) expression difference of over twofold. Duplicate gene symbols indicate multiple probe sets for the same gene; a number is included at far left only for the first instance of each.

Figure 2 Naive CD5^{lo} and CD5^{hi} CD8⁺ T cells have distinct gene-expression characteristics. **(a)** Expression of XCL1 (right) by a memory phenotype (CD44^{hi}) CD8⁺ T cell population (far right) and by naive (CD44^{lo}) CD8⁺ T cells among splenocytes left unstimulated (US) or stimulated (PMA + iono) with the phorbol ester PMA and ionomycin in the presence of brefeldin A and then stained intracellularly for XCL1, gated on CD5 expression (as in **Fig. 1a,b**). Numbers adjacent to outlined areas (far left) indicate percent CD44^{hi}CD8^{hi} cells (top) or CD44^{lo}CD8^{hi} cells (bottom); numbers above bracketed lines (right) indicate percent XCL1⁺ cells. **(b)** Frequency of cells of various subsets (key) expressing XCL1, assessed following activation as in **a**, or expressing CXCR3 or T-bet, assessed in unstimulated cells pooled from C57BL/6 (B6) mice and T-bet reporter mice (in which GFP is expressed under control of the gene encoding T-bet)⁵⁰. **(c)** Ratio of the expression of genes in clusters II, III and X by CD5^{lo} cells relative to their expression in CD5^{hi} cells, among CD44^{lo} CD8⁺ T cells gated on CD5 expression (as in **Fig. 1a,b**); gene-expression data were aligned with gene clusters that are associated with stages of the *in vivo* CD8⁺ T cell response³⁴. A ratio of <1 (left of the vertical dashed line) indicates 'preferential' expression in the CD5^{hi} population. **P* < 0.001 (unpaired *t*-test). Data are representative of four experiments with nine mice (**a**) or are from four experiments (*n* = 9 mice) for XCL1, three experiments (*n* = 7 mice) for T-bet or five experiments (*n* = 13 mice) for CXCR3 (**b**; error bars, s.e.m.) or three independent experiments (**c**).



compare differences in gene transcription by CD5^{hi} and CD5^{lo} cells with a database generated by Immunological Genome Project Consortium, which has comprehensively defined patterns of gene expression after the activation and differentiation of CD8⁺ T cells³⁴. In that work, temporal analysis of gene expression over the course of the immune response allowed the characterization of ten clusters of correlated gene expression (clusters I–X)³⁴. We investigated how expression of genes in these clusters was regulated in the CD5^{hi} and CD5^{lo} naive CD8⁺ T cell subsets. This analysis revealed that the CD5^{hi} population expressed a significantly higher proportion of genes that characterize two early stages of the CD8⁺ T cell response and are associated with preparation for cell cycle (cluster II) and active cell cycle and division (cluster III) (**Fig. 2c** and **Table 2**). We also found a more moderate (but still highly significant) correlation of genes 'preferentially' expressed in the CD5^{hi} population with cluster X, which defines genes expressed at late effector and memory stages (**Fig. 2c** and **Table 2**). Together these data suggested the CD5^{hi} population would be better poised for initial activation than the CD5^{lo} population.

Enhanced expansion of the CD5^{hi} population after infection

We next directly investigated whether CD5^{hi} and CD5^{lo} naive CD8⁺ T cells differed in their primary immune response to foreign antigen. In initial studies, we assayed polyclonal CD8⁺ T cells specific for the H-2K^b-restricted epitope derived from amino acids 20–27 of the vaccinia virus glycoprotein B8R (peptide called simply 'B8R' here), which are present at a frequency of ~1 cell per 1 × 10⁴ to 2 × 10⁴ CD8⁺ T cells in unimmunized C57BL/6 mice³⁵. We sorted naive CD44^{lo} CD8⁺ T cells by flow cytometry into congenically distinct CD5^{lo} and CD5^{hi} populations and transferred ~1.5 × 10⁶ cells of each population together into congenic wild-type recipient mice that we subsequently infected with LM-B8R, a recombinant attenuated *Listeria monocytogenes* strain that expresses the B8R epitope and the H-2K^b-restricted peptide of ovalbumin amino acids 257–264 (called simply 'OVA' here). With the assumption of ~20% engraftment following adoptive transfer, this would be expected to seed ~20 B8R–H-2K^b-specific cells from each donor. At day 7 following infection, we used staining with peptide-MHC (pMHC) tetramers to identify responsive CD5^{hi} and CD5^{lo} donor cells

and determined the ratio (**Fig. 3a**) and absolute number (**Fig. 3b**) of each population. In most cases, the CD5^{hi} donor population dominated the response, on average accounting for ~95% of the B8R–H-2K^b-specific population (**Fig. 3a,b**), although occasionally progeny of the CD5^{lo} donor cells were more frequent (**Fig. 3a,b**). Tetramer binding may fail to identify all functionally responsive cells, but we obtained similar results by using peptide-induced production of interferon- γ to identify antigen-specific T cells (**Supplementary Fig. 3a,b**). At the memory phase following priming and also during a recall response, the progeny of CD5^{hi} donor cells maintained dominance over those from the CD5^{lo} pool (**Fig. 3a**). The finding that this skewing was not exacerbated during the recall response indicated that memory cells generated from CD5^{lo} and CD5^{hi} cells had similar population-reexpansion potential.

The dominance of CD5^{hi} naive CD8⁺ T cell responses was not unique to B8R–H-2K^b-specific T cells or to infection with *L. monocytogenes*: The OVA–H-2K^b-specific response induced by infection with LM-B8R, as well as the response specific to the H-2D^d-restricted epitope from lymphocytic choriomeningitis virus (LCMV) glycoprotein amino acids

Table 2 Differences in the induction of CD8⁺ T cell gene-expression clusters

Cluster	Characteristics	CD5 ^{lo}	CD5 ^{hi}	<i>P</i>	Proportion
I	Initial cytokine or effector response	12	22	0.086	0.352
II	Preparation for cell division	187	334	1.193 E-10	0.358
III	Cell cycle & division	93	187	1.936 E-08	0.332
IV	Naive and late memory	51	40	0.248	0.560
V	Early effector, late memory	54	72	0.108	0.428
VI	Short-term effector and memory	27	37	0.211	0.421
VII	Memory precursor	61	49	0.252	0.554
VIII	Naive or late effector or memory	129	138	0.581	0.483
IX	Short-term effector or memory	39	55	0.098	0.414
X	Late effector or memory	34	59	0.009	0.365

Differences in the expression of gene-expression clusters by CD5^{hi} and CD5^{lo} naive CD8⁺ T cells and that of gene-set clusters (far left) by CD8⁺ T cells assessed by the Immunological Genome Project (published clusters and designated characteristics³⁴). Values in columns 'CD5^{lo}' and 'CD5^{hi}' indicate the number of genes in each cluster that were 'preferentially' expressed in that subset; 'Proportion' indicates the fraction of those genes expressed in the CD5^{lo} subset; the significance of differences in expression was calculated by the χ^2 test (*P*).

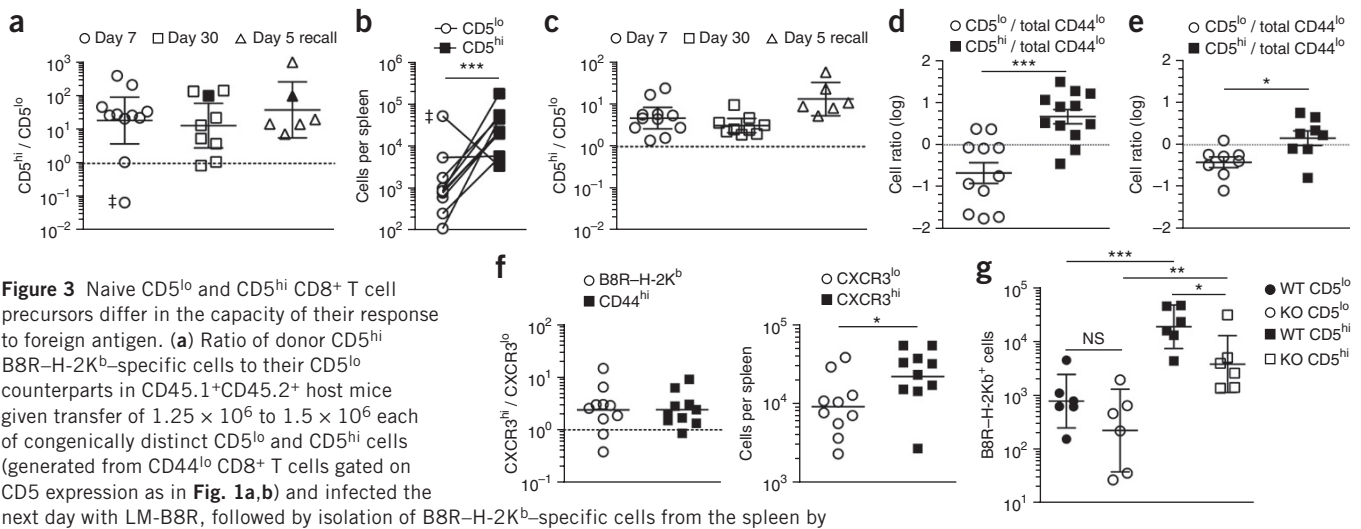


Figure 3 Naive CD5^{lo} and CD5^{hi} CD8⁺ T cell precursors differ in the capacity of their response to foreign antigen. **(a)** Ratio of donor CD5^{hi} B8R-H-2K^b-specific cells to their CD5^{lo} counterparts in CD45.1⁺CD45.2⁺ host mice given transfer of 1.25×10^6 to 1.5×10^6 each of congenically distinct CD5^{lo} and CD5^{hi} cells (generated from CD44^{lo} CD8⁺ T cells gated on CD5 expression as in Fig. 1a,b) and infected the next day with LM-B8R, followed by isolation of B8R-H-2K^b-specific cells from the spleen by B8R-H-2K^b tetramer enrichment and analysis at day 7 or 30 after primary infection or 5 d after rechallenge of recipient mice (at >30 d after the primary infection) with virulent LM-B8R (Day 5 recall). Filled symbols indicate mice for which a B8R-H-2K^b-specific response was not detected for CD5^{lo} donor cells and the ratio was arbitrarily set as 10². **(b)** Total donor cells at day 7 in mice as in a. Each symbol represents an individual mouse; ‡ indicates an outlier (exclusion of this group did not alter the significance of these results). **(c)** Ratio of bulk LM-B8R-specific donor CD5^{hi} CD8⁺ T cells to their CD5^{lo} counterparts in mice as in a. **(d,e)** B8R-H-2K^b-specific responses **(d)** and bulk LM-B8R-specific responses **(e)** in congenic recipients given a mixture of sorted CD8⁺ CD44^{lo} cells plus congenically distinct CD44^{lo} CD5^{lo} or CD44^{lo} CD5^{hi} populations (1.25×10^6 to 1.5×10^6 cells of each population), followed by infection of recipients with LM-B8R 1 d later and analysis 7 d after infection. **(f)** Ratio of cells derived from CXCR3^{lo} donor cells to their CXCR3^{hi} counterparts in the B8R-H-2K^b-specific and bulk LM-B8R-responsive populations (left), and quantification of B8R-H-2K^b-specific CXCR3^{hi} and CXCR3^{lo} donor cells (right), in CD45.1⁺CD45.2⁺ recipients given 1×10^6 to 2×10^6 congenically distinct CXCR3^{lo} or CXCR3^{hi} CD5^{hi} cells (CD5^{hi} naive CD8⁺ T cells (CD44^{lo} cells in the top 20% for CD5 expression) sorted as cells with the lowest or highest 30% of CXCR3 expression), followed by infection of recipients with LM-B8R 1 d later and isolation of B8R-H-2K^b-specific cells from the spleen 7 d after infection by tetramer enrichment. **(g)** Quantification of B8R-H-2K^b-specific donor cells in the spleen of congenic recipients given congenically distinct combinations of wild-type (WT) and CD25 (IL-2R α)-deficient (KO) CD44^{lo} CD5^{lo} and CD5^{hi} cells sorted from chimeras reconstituted with congenic wild-type and CD25 (IL-2R α)-deficient bone marrow, followed by infection of recipients with LM-B8R 1 d later and analysis at day 7 following infection. Each symbol represents an individual mouse; small horizontal lines indicate the geometric mean **(a,c,f)** or mean **(d,e,g)** (\pm 95% confidence interval in **a,c,g** or \pm s.e.m. in **d,e,g**). NS, not significant; * $P < 0.05$, ** $P < 0.01$ and *** $P < 0.001$ (unpaired *t*-test). Data were pooled from four experiments at day 7 ($n = 11$ mice), three experiments at day 30 ($n = 9$ mice) or two experiments for day 5 recall ($n = 6$ mice) **(a-c)**, three experiments **(d,f)**, $n = 11-12$ mice **(d)** or $n = 10$ mice **(f)** or three independent experiments ($n = 6$ mice) **(g)** or are from two experiments ($n = 8$ mice) **(e)**.

33–41 (gp33), induced by infection with LCMV, were also biased to the CD5^{hi} donor cells (**Supplementary Fig. 3c,d**). Beyond individual antigen specificities, the bulk pathogen-specific response, identified as donor CD8⁺ T cells that had acquired an antigen-experienced CD44^{hi}CD8^{lo}CD11a^{hi} phenotype, also showed an advantage for the CD5^{hi} donor pool, albeit less pronounced than that observed for individual pMHC-specific responses (**Fig. 3c** and **Supplementary Fig. 3e**).

The ‘preferential’ expansion of the CD5^{hi} donor population did not reflect a greater intrinsic capacity of these cells for TCR-induced proliferation, as CD5^{lo} and CD5^{hi} naive CD8⁺ T cells proliferated similarly upon *in vitro* stimulation with antibody to the invariant signaling protein CD3 (anti-CD3) plus antibody to the coreceptor CD28 (anti-CD28) (**Supplementary Fig. 3f**), consistent with published studies^{9,20,24}. We also noted the enhanced CD5^{hi} T cell B8R-H-2K^b-specific response in studies of recipient mice deficient in recombination-activating gene 1, which are deficient in mature B cells and T cells (**Supplementary Fig. 3g**); this ruled out the possibility of a required contribution from host T lymphocytes or B lymphocytes.

Since naive CD5^{hi} cells have intermediate expression of CD44, it was formally possible that some memory-phenotype T cells had contaminated the CD5^{hi} donor population. However, when we sorted CD5^{hi} and CD5^{lo} donor populations to have equally low CD44 expression, the CD5^{hi} donor population still dominated the response to LM-B8R (**Supplementary Fig. 3h**), which argued against the possibility of contamination by memory cells in our studies. The differences in the responses of CD5^{hi} and CD5^{lo} naive CD8⁺ T cells suggested that

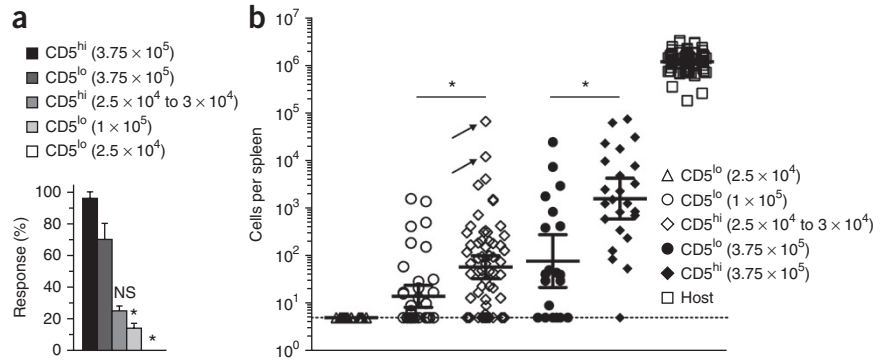
reactivity improved proportionally to increasing CD5 expression. To explore this, we measured the response of CD5^{lo} and CD5^{hi} populations to infection, relative to that of the total naive CD8⁺ T cell pool (containing the full spectrum of CD5 expression). The CD5^{lo} population expanded less than bulk naive CD8⁺ T cells did, while the CD5^{hi} cells proliferated more (**Fig. 3d,e**), which suggested that CD5^{lo} and CD5^{hi} populations represent the extremes of a continuum in reactivity to foreign antigen.

Given that the CD5^{hi} population was heterogeneous (**Fig. 2b** and **Supplementary Fig. 2c**), it was possible that a small subset within this pool was responsible for their superior antigen-specific responses. We investigated this hypothesis by subdividing the naive CD5^{hi} population on the basis of CXCR3 expression, since this chemokine receptor has been associated with enhanced detection of antigen *in vivo* by memory CD8⁺ T cells^{36,37}. We sorted congenic populations of naive CD5^{hi} cells into CXCR3^{lo} and CXCR3^{hi} populations and assessed their response toward infection with LM-B8R using the co-transfer model described above. We observed that expansion of the CXCR3^{hi} CD5^{hi} population was significantly greater than that of the CXCR3^{lo} CD5^{hi} subset, in both the B8R-H-2K^b-specific responder population and bulk CD44^{hi} responder population (**Fig. 3f**). However, these differences were of lower magnitude than those between the CD5^{hi} and CD5^{lo} populations (**Fig. 3a,b,f**), which challenged the hypothesis that a small subset of CD5^{hi} cells accounted for all the enhanced reactivity of this population.

In addition to being influenced by TCR signals, CD8⁺ T cell responses are strongly influenced by cytokines. Naive CD5^{hi} CD8⁺

Figure 4 Analysis of the clonal responses of naive CD5^{lo} and CD5^{hi} CD8⁺ T cells to infection.

(a) Response rate of B8R–H-2K^b-specific donor cells (above the limit of detection of five cells) in the spleen of congenic recipients given sorted CD5^{lo} or CD5^{hi} cells (number of cells transferred, key), followed by infection of recipients with LM-B8R and analysis 7 d after infection (congenic marker scheme, **Supplementary Fig. 4**). NS, not significant ($P = 0.2$), response rate for 2.5×10^4 to 3.0×10^4 CD5^{hi} cells versus expected response (~27.5%), and $*P < 0.0001$, response rate of 2.5×10^4 CD5^{lo} cells (0/40) or 1×10^5 CD5^{lo} cells (18/125) versus expected response (25% or 100%, respectively) (one-sided binomial test). (b) Quantification of B8R–H-2K^b-specific CD8⁺ T cells derived from each donor population in a, as well as responses of host cells (key), presented as log-transformed values; horizontal dashed line indicates limit of detection (donor populations that did not mount a detectable response are grouped on that line); arrows indicate largest CD5^{lo} clonal response. Each symbol represents an individual donor cohort; small horizontal lines indicate the geometric mean (\pm 95% confidence interval). $*P < 0.05$, for responses above the limit of detection (Mann-Whitney test). Data are from two to four independent experiments (error bars (a), s.d.).



T cells are more reactive to common γ -chain cytokines than are their CD5^{lo} counterparts^{24,26}, and they have enhanced ability to produce IL-2 following stimulation via the TCR¹¹, which might induce autocrine signaling via IL-2R. Also, the ability of inflammatory cues to augment the magnitude of CD8⁺ T cell responses involves sustained expression of the T cell activation–marker (and cytokine receptor chain) CD25 (ref. 38). To determine whether CD25 expression affected the differences in responses of CD5^{lo} and CD5^{hi} naive CD8⁺ T cells, we assessed the reactivity of CD25-deficient polyclonal CD8⁺ T cells, generated in mixed–bone marrow chimeras to avoid the lymphoproliferation and autoimmunity of CD25-deficient mice³⁹. The distribution of CD5 expression was similar in wild-type and *Cd25*^{-/-} resting naive CD8⁺ T cells (**Supplementary Fig. 3i**). As expected, the B8R–H-2K^b-specific wild-type CD5^{hi} population expanded more than the wild-type CD5^{lo} population did (**Fig. 3g**), but, while CD25 deficiency did not have a significant effect on the response of B8R–H-2K^b-specific CD5^{lo} cells, the response of *Cd25*^{-/-} CD5^{hi} cells was modestly but significantly impaired (**Fig. 3g**). While these data suggested the CD5^{hi} pool might have been more reliant on responsiveness to IL-2, the responses of CD5^{hi} and CD5^{lo} cells were not ‘normalized’ by CD25 deficiency, which indicated that elevated sensitivity to IL-2 could not fully account for the differences between these populations. Together these data indicated that the antigen-specific response to pathogens was dominated by CD5^{hi} naive CD8⁺ T cells.

Distinct clonal responses of CD5^{hi} versus CD5^{lo} CD8⁺ T cells

Our analyses of bulk naive CD8⁺ T cell responses were unable to determine whether the differences in the expansion of CD5^{hi} and CD5^{lo} naive CD8⁺ T cell populations reflected enhanced responses by all antigen-reactive CD5^{hi} cells or dominance by a small number of CD5^{hi} CD8⁺ T cell clones. This is relevant because the expansion characteristics of progeny from individual antigen-specific naive T cells can vary considerably^{2,4,40–42}. Accordingly, we reduced the number of adoptively transferred naive CD44^{lo} CD5^{hi} or CD5^{lo} polyclonal naive CD8⁺ T cells to 25×10^3 to 30×10^3 cells. Given the frequency of B8R–H-2K^b-specific precursor cells³⁵, 20% engraftment would seed approximately one B8R–H-2K^b-specific donor CD8⁺ T cell per three to five donor cell cohorts, which would result in an average predicted response rate of ~27.5%. To increase the efficiency of detecting a clonal response, we used simultaneous transfer of up to eight congenically distinct donor populations into a single recipient, as described before^{2,4,40} (**Supplementary Fig. 4**). In studies of

CD5^{hi} naive CD8⁺ T cells, ~24% (46 of 188) of the transfers led to a B8R–H-2K^b-specific response, which was not significantly different from the predicted frequency (**Fig. 4a**) and was consistent with studies of naive OT-I T cells⁴⁰. In contrast, adoptive transfer of 25×10^3 CD5^{lo} cells led to no detectable B8R–H-2K^b-specific donor responses (0 of 40 transfers), which was significantly below the predicted rate (**Fig. 4a**). Increasing the input of CD5^{lo} donor cells to 100×10^3 led to detectable responses, but only in 14% (18 of 125) of transfers (**Fig. 4a**). This response rate suggested that less than one seventh of the expected number of CD5^{lo} CD8⁺ T cell precursors were able to mount a detectable response. Examination of nonclonal responses by 375×10^3 CD5^{hi} or CD5^{lo} donor cells showed that >95% of CD5^{hi} cells mounted a response (23 of 24 transfers), but only 70% of donor CD5^{lo} cells did so (14 of 20 transfers) (**Fig. 4b**), which further demonstrated the reduced response rate of the CD5^{lo} pool.

Furthermore, the mean magnitude of the clonal expansion (‘burst size’) of the responding CD5^{lo} population (from the transfer of 100×10^3 cells) was significantly smaller than that of the CD5^{hi} population (from the transfer of 25×10^3 to 30×10^3 cells) (**Fig. 4b**). It was also notable that the two largest clonal responses were derived from CD5^{hi} precursor cells and were 10- to 100-fold greater than the largest CD5^{lo} clonal response (**Fig. 4b**). Modeling of the outcome if all the CD5^{hi} and CD5^{lo} clonal responses measured had occurred in a single mouse showed that those two clones would account for nearly 80% of the B8R–H-2K^b-specific population (data not shown).

Hence, clonal analysis revealed two ways in which the responses of CD5^{hi} and CD5^{lo} T cells differed. First, the CD5^{hi} population displayed a markedly greater response rate. Second, even among cells that did engage in the B8R–H-2K^b-specific response, the average clonal burst size from the CD5^{lo} pool was less than that from the CD5^{hi} pool. Together, these differences accounted for much of the expansion advantage of the CD5^{hi} pool.

Efficient recruitment of CD5^{hi} CD8⁺ T cell responses

The greater clonal recruitment of CD5^{hi} cells than of CD5^{lo} cells might have reflected ‘preferential’ initial activation of CD5^{hi} cells or a similar initial response by both populations, followed by improved proliferation and/or survival of the CD5^{hi} population. The superior response by CD5^{hi} cells was already apparent at days 3–4 of the *in vivo* response to LM-B8R (**Fig. 5a**); hence, we next investigated whether CD5^{hi} cells were ‘preferentially’ activated during the initial response to infection. This was not feasible by adoptive transfer of polyclonal

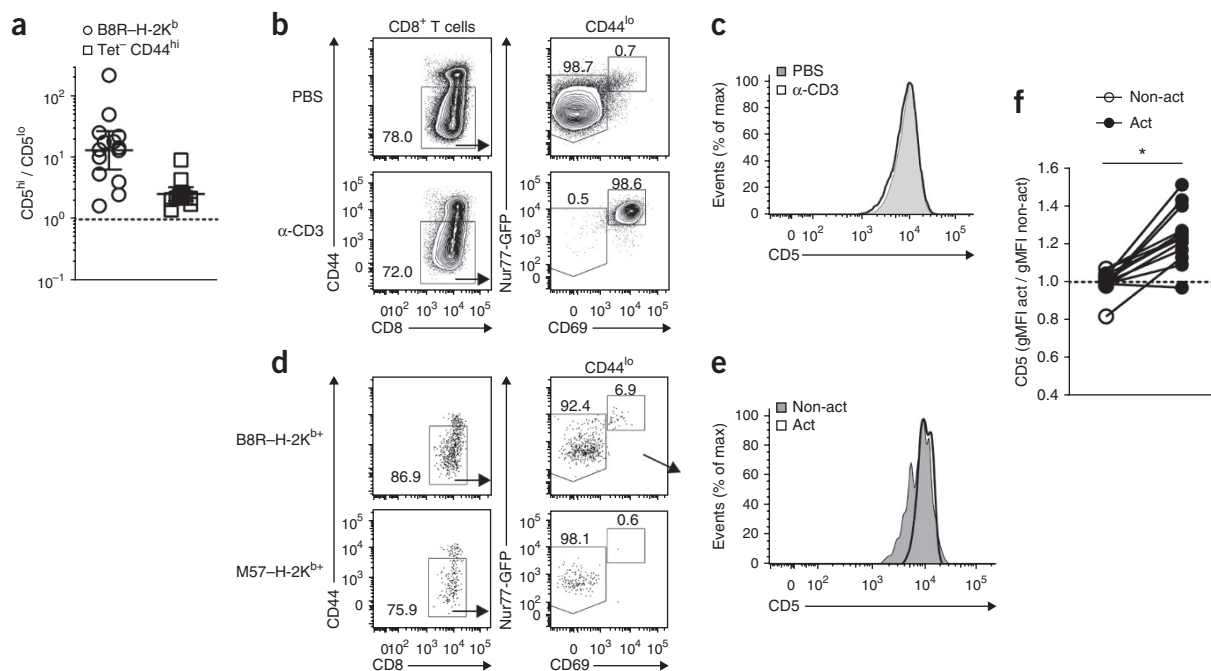


Figure 5 Early recruitment of CD5^{lo} and CD5^{hi} cells into the immune response after infection. **(a)** Responses of donor-derived B8R–H-2K^b-specific cells (assessed as in Fig. 3a) in the spleen of congenic recipients given congenically distinct CD44^{lo} CD5^{lo} and CD5^{hi} cells (sorted and transferred together as in Fig. 3), followed by infection of recipients with LM-B8R and analysis on day 3 or 4 after infection. Each symbol represents an individual recipient mouse; small horizontal lines indicate the geometric mean (\pm 95% confidence interval). **(b,c)** Expression of Nur77-GFP and CD69 **(b)** and CD5 **(c)** on CD44^{lo} CD8⁺ T cells in the spleen of *Nur77*^{GFP} mice 5 h after intravenous injection of 50 μ g anti-CD3 (α -CD3) or PBS. **(d)** Expression of Nur77-GFP and CD69 on B8R–H-2K^b- or M57–H-2K^b-specific CD8⁺ T cells isolated by tetramer-based enrichment from the spleen of *Nur77*^{GFP} mice 5 h after infection with 1×10^7 colony-forming units of LM-B8R. **(e)** CD5 expression by B8R–H-2K^b-specific cells obtained as in **d**, with a non-activated (Non-act) (*Nur77*-GFP^{lo}CD69⁻) or activated (act) (*Nur77*-GFP^{hi}CD69⁺) phenotype. **(f)** CD5 expression on non-activated and activated B8R–H-2K^b-specific naive CD8⁺ T cells as in **e**, presented as geometric mean fluorescence intensity (gMFI). Numbers adjacent to outlined areas **(b,d)** indicate percent CD44^{lo}CD8⁺ cells (left plots) or Nur77-GFP^{lo}CD69⁻ cells (left) or Nur77-GFP^{hi}CD69⁺ cells (right) (right plots). **P* < 0.01 (unpaired *t*-test). Data are pooled from three experiments (one at day 3 (*n* = 5 mice) and two at day 4 (*n* = 9 mice)) **(a)**, are from three independent experiments (*n* = 6 mice) **(b,c)** or are representative of or pooled from three experiments for B8R–H-2K^b-specific cells (*n* = 13 mice) or two experiments for M57–H-2K^b-specific cells (*n* = 9 mice) **(d-f)**.

cells, and to determine the response of endogenous CD5^{hi} and CD5^{lo} cells, it was first necessary to determine whether CD5 expression changed during short-term activation *in vivo*. We gave *Nur77*^{GFP} mice intravenous injection of anti-CD3 and, 5 h later, assessed T cell activation as induction of expression of the activation marker CD69 and *Nur77*^{GFP} (as indicated by expression of the protein encoded (*Nur77*-GFP)). Despite robust activation, naive CD8⁺ T cells showed no change in CD5 expression (Fig. 5b,c), which indicated that CD5^{hi} and CD5^{lo} naive populations could still be distinguished. Next we infected *Nur77*^{GFP} mice with LM-B8R and, 5 h later, enriched splenic CD8⁺ T cell populations specific for B8R–H-2K^b and for an irrelevant antigen (the H-2K^b-restricted epitope from amino acids 816–824 of mouse cytomegalovirus protein M57 (M57–H-2K^b)) by capture with MHC class I tetramers. Following infection with LM-B8R, activated naive CD8⁺ T cells were evident among the B8R–H-2K^b-specific population but not among the control M57–H-2K^b-specific population (Fig. 5d), and the activated B8R–H-2K^b-specific population showed enrichment for CD5^{hi} cells (Fig. 5e,f). These data suggested that initial recruitment and/or activation favored the CD5^{hi} naive CD8⁺ T cell pool during the response to foreign antigen.

Similar TCR-binding characteristics of CD5^{lo} and CD5^{hi} cells

Some studies have suggested that CD5 expression on naive CD4⁺ T cells with transgenic TCR expression correlates with the affinity of the TCR for foreign peptide–MHC, indicated by greater labeling of

CD5^{hi} clones than CD5^{lo} clones with pMHC tetramers⁹. However, we found similar intensities of staining with pMHC tetramers on CD5^{hi} and CD5^{lo} naive CD8⁺ T cell populations isolated from unimmunized mice by tetramer enrichment (Fig. 6a), which suggested similar capacities for binding foreign peptide–MHC ligands. Furthermore, the intensity of staining with B8R–H-2K^b tetramers was not significantly different on effector cells derived from clonal CD5^{lo} responses and those derived from CD5^{hi} responses, which revealed that intensity did not differ significantly for antigen-specific progeny of CD5^{lo} clones versus those of CD5^{hi} clones, whereas the burst size of CD5^{hi} clones was significantly greater than that of CD5^{lo} clones (Fig. 6b). Thus, we observed minimal correlation between the intensity of staining with pMHC tetramers and either CD5 expression or clonal-expansion characteristics of specific CD8⁺ T cells.

It was also possible that foreign antigen–specific T cells were selectively under-represented in the CD5^{lo} pool. We did observe modest, but in some cases significant, skewing toward higher CD5 expression in the pool of naive CD8⁺ T cells that bound foreign peptide–MHC tetramers (Fig. 6c) and, accordingly, there were slightly more B8R–H-2K^b-specific cells in sorted CD5^{hi} populations than in sorted CD5^{lo} populations (Supplementary Fig. 5). However, such skewing contributed an average increase of only ~1.5-fold in antigen-specific precursor cells in the CD5^{hi} population, relative to that in the CD5^{lo} population (Supplementary Fig. 5), which could not explain the larger differences in the clonal recruitment or

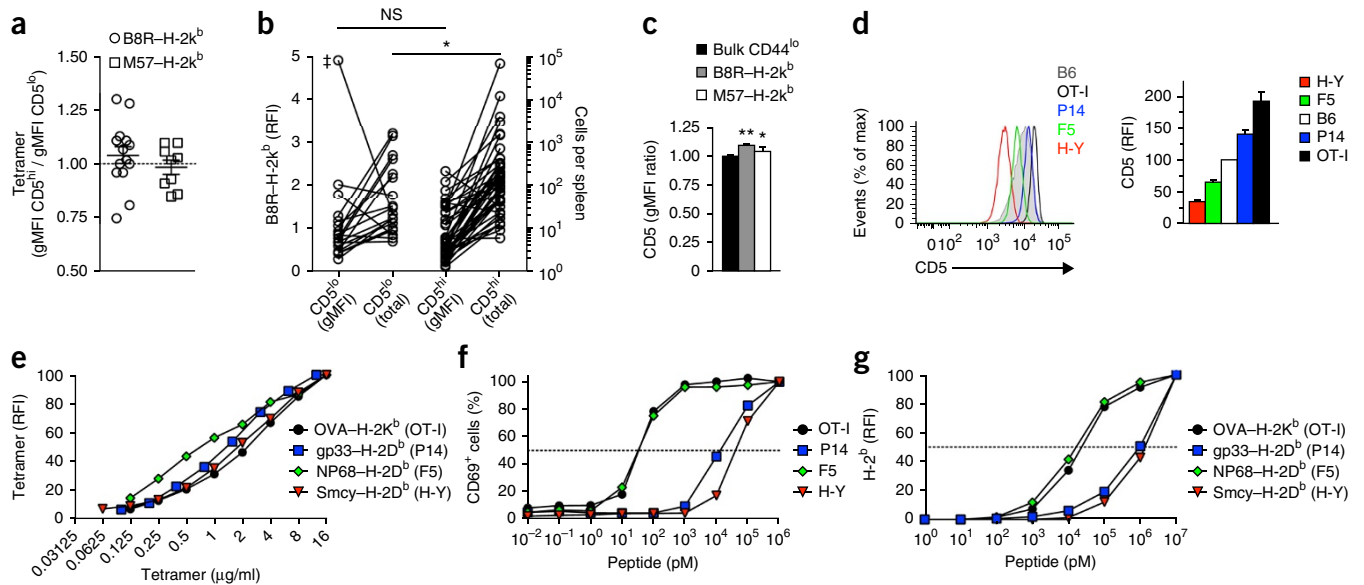


Figure 6 CD5^{hi} and CD5^{lo} cells show similar binding of the TCR to cognate antigen. (a) Tetramer-staining intensity of B8R-H-2K^b- and M57-H-2K^b-specific CD8⁺ T cells (key) enriched from unimmunized mice with gating of CD44^{lo} precursor cells on the lower and upper 20% of CD5 expression; results are presented as a ratio (CD5^{hi}/CD5^{lo}) to normalize results. Each symbol represents an individual mouse; small horizontal lines indicate the mean (\pm s.e.m.). (b) B8R-H-2K^b tetramer staining (left vertical axis) and burst size (right vertical axis) of expanded clonal populations derived from donor cells in recipient mice given 1×10^5 CD5^{lo} cells and 2.5×10^4 to 3.0×10^4 CD5^{hi} cells (as in Fig. 4), followed by infection of host mice with LM-B8R and analysis at day 7 after infection; tetramer staining on donor cells was normalized to that on B8R-H-2K^b-specific host cells from the same mouse to yield relative fluorescence intensity (RFI). †, outlier. (c) CD5 expression on bulk CD44^{lo} CD8⁺ T cells and B8R-H-2K^b-specific and M57-H-2K^b-specific CD44^{lo} CD8⁺ T cell populations (key) isolated by tetramer enrichment from the spleen and lymph nodes of unimmunized mice. (d) CD5 expression on CD8⁺ T cells from C57BL/6 mice (B6) and various strains of mice with transgenic expression of MHC class I-restricted TCRs (key); right, results normalized to the average expression on the bulk CD44^{lo} population and are presented relative to those of polyclonal C57BL/6 CD44^{lo} CD8⁺ T cells (B6), set as 100. (e) Binding of various concentrations of MHC class I tetramers (horizontal axis) to cells of strains as in d (in parentheses in key), presented relative to maximum intensity, set as 100. (f) CD69 expression (*in vitro* activation) of CD8⁺ T cells obtained from mice of strains as in d (key), then incubated for 6 h with titrated doses of peptide (horizontal axis), assessed by flow cytometry; results are presented relative to maximum CD69 expression, set as 100% (horizontal dotted line indicates 50% response). (g) Expression of H-2K^b or H-2D^b (H-2^b) on RMA-S mouse tumor cells incubated with various doses (horizontal axis) of the peptide recognized by the TCR transgenically expressed by each strain of T cell (key); results are presented as staining of MHC class I relative to maximum staining intensity, set as 100 (horizontal dotted line indicates 50% of maximum). (h) CD5 expression by host CD44^{lo} cells or donor OT-I cells (key) from congenic recipients of 1×10^3 cells of each population (wild-type or mutant) of congenically distinct CD44^{lo} OT-I CD8⁺ T cells enriched from chimeras (generated by transfer of OT-I bone marrow into irradiated wild-type (WT) or β_2 -microglobulin-deficient (*B2m*^{-/-}) hosts), followed by no further treatment of recipients or infection 1–3 d later with attenuated OVA-expressing *L. monocytogenes* Δ actA (Δ actA LM-OVA) (diagram at right). (i) Ratio of CD5^{hi} OT-I donor cell populations to CD5^{lo} OT-I donor cell populations, normalized to the average ratio of engraftment ('take') in uninfected recipients (Day 0), and at 7 d and 12 d after infection with OVA-expressing *L. monocytogenes* as in h. Each symbol represents an individual mouse; small horizontal lines indicate the mean (\pm s.e.m.). NS (b), $P > 0.05$, with or without inclusion of the outlier (†); * $P < 0.05$ (unpaired *t*-test (b) and ** $P < 0.001$ (paired *t*-test (c)). Data were pooled from four experiments ($n = 14$ mice (B8R-H-2K^b) or $n = 9$ mice (M57-H-2K^b)) (a), are from at least three experiments with 18 (CD5^{lo}) or 46 (CD5^{hi}) clonal responses (b), were pooled from six experiments for B8R-H-2K^b-specific cells ($n = 21$ mice) or two experiments for M57-H-2K^b-specific cells ($n = 8$ mice) (c; mean and s.e.m.), were pooled from two to three experiments ($n = 4$ –6) (d; mean and s.e.m.), are from one experiment representative of two independent experiments with similar results (e,f), are representative of three independent experiments (g) or are from one experiment with four independent sets of chimeras (h,i).

population expansion of antigen-specific CD5^{hi} cells relative to that of CD5^{lo} cells (Figs. 3 and 4).

To avoid potential artifacts from the tetramer-enrichment protocol, we analyzed four lines of mice with transgenic TCR expression that differ in surface expression of CD5, in the order H-Y < F5 < P14 < OT-I (lowest to highest CD5 expression)^{22,23,26} (Fig. 6d). All the strains bound cognate pMHC tetramers with similar efficiency in dose titration (Fig. 6e), which indicated that in contrast to studies of CD4⁺ T cells with transgenic TCR expression⁹, low CD5 expression versus high CD5 expression could not be used to predict the strength of the binding of foreign peptide-MHC ligands to CD8⁺ T cells

with transgenic TCR expression. Interpreting tetramer staining may be complicated by the findings that the expression of CD8 and TCR was lower on CD5^{hi} naive CD8⁺ T cells than on CD5^{lo} naive CD8⁺ T cells (Supplementary Fig. 1a) and that CD8 contributes to binding of peptide-MHC class I tetramers⁴³. Hence, we also assessed the reactivity (as induction of CD69 expression) of CD5^{hi} and CD5^{lo} T cells with transgenic TCR expression to their cognate foreign ligands in response to dose titration. Although we noted differences in antigen sensitivity, they did not correlate with the level of CD5 expression; for example, CD5^{hi} OT-I CD8⁺ T cells and CD5^{lo} F5 CD8⁺ T cells showed similar antigen sensitivity (Fig. 6f). Instead,

Figure 7 CD5^{hi} cells ‘preferentially’ use proinflammatory signals during population expansion. **(a)** Total donor CD8⁺ T cells in the spleen of congenic recipients of a mixture of congenically distinct CD44^{lo} H-Y and OT-I CD8⁺ T cells (key), followed by immunization of recipients the next day with a mixture of matured DCs that were independently pulsed with OVA or C2A, with (DC + LM) or without (DC alone) infection with *L. monocytogenes* Δ actA and analysis 7 d later. **(b)** Ratio of OT-I cells to H-Y cells 1 d after adoptive transfer as in **a**, normalized to the ‘take’ ratio in unimmunized mice. **(c)** Total donor CD8⁺ T cells congenic recipients immunized as in **a**, with (DC + LCMV) or without (DC alone) infection with LCMV Armstrong strain. **(d)** Ratio of OT-I cells to H-Y cells 1 d after adoptive transfer as in **c**, normalized as in **b**. **P* < 0.01 and ***P* < 0.001 (unpaired *t*-test). Data are pooled from three independent experiments (*n* = 10 mice) (**a,b**; mean and s.e.m.) or are from two experiments (*n* = 6 mice (DC alone) or *n* = 7 mice (DC + LCMV)) (**c,d**; mean and s.e.m.).

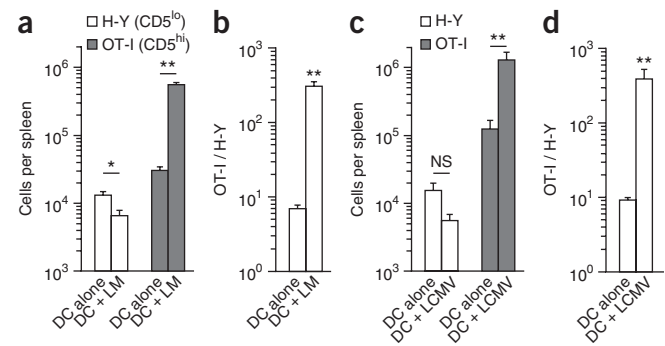
dose sensitivity corresponded with binding of peptide to the relevant MHC molecules (**Fig. 6g**). Hence, these data indicated that CD5 expression could not be used to predict tetramer binding or *in vitro* antigen sensitivity of naive CD8⁺ T cells.

An expectation from our findings would be that CD5^{hi} and CD5^{lo} naive CD8⁺ T cells with identical TCRs would display distinct response characteristics. This hypothesis was supported by published studies of CD8⁺ T cells with transgenic TCR expression, sorted into CD5^{hi} and CD5^{lo} pools²⁴, but as CD5 levels are typically determined during thymic development, we sought to manipulate positive selection to produce cells with distinct levels of CD5 expression. We generated chimeras by reconstituting wild-type or β_2 -microglobulin-deficient hosts with OT-I donor marrow; in the latter hosts, positive selection is mediated by hematopoietic cells, which resulted in generation of OT-I cells with lower CD5^{lo} expression (**Fig. 6h** and data not shown). When we assessed their response to infection with OVA-expressing *L. monocytogenes*, we found that the CD5^{hi} OT-I population expanded approximately three- to fourfold more than the CD5^{lo} OT-I population (**Fig. 6i**), which indicated that the level of CD5 expression correlated with the magnitude of the immune response, even when TCR specificity was normalized. In aggregate, our data suggested that the advantage of CD5^{hi} naive CD8⁺ T cells over CD5^{lo} naive CD8⁺ T cells in their response to foreign antigen could not be explained by differences in precursor frequency or avidity for foreign peptide-MHC ligands.

Use of inflammatory cues by CD5^{hi} CD8⁺ T cells

In addition to being influenced by TCR signals, the magnitude of the CD8⁺ T cell response is influenced by inflammatory cues^{44,45}; hence, we next assessed the effect of inflammation on the response of CD5^{hi} and CD5^{lo} naive CD8⁺ T cells. Since the population expansion of CD8⁺ T cells is reduced in the absence of innate cues^{46,47}, this system was not suitable for analysis of rare antigen-specific polyclonal CD8⁺ T cells; hence, we used H-Y T cells and OT-I T cells as examples of CD5^{lo} clones and CD5^{hi} clones, respectively. We transferred small numbers of H-Y and OT-I naive CD8⁺ T cells into congenic hosts and stimulated the cells by injection of DCs loaded with cognate peptides, with or without simultaneous infection with the attenuated *L. monocytogenes* strain Δ actA (which expresses no stimulatory antigens for either transgenically expressed TCR) as a source of inflammatory stimulation. We used OVA to stimulate OT-I cells, while we stimulated H-Y T cells with C2A, a variant of the Smcy peptide that enhances recognition of the H-Y TCR without altering MHC binding⁴⁸ (**Supplementary Fig. 6a–c**), to minimize differences in the sensitivity of H-Y and OT-I T cell clones to ligand dose.

As expected, antigen-bearing DCs alone elicited modest responses by both H-Y cells and OT-I cells (**Fig. 7a**) and, after correction for



donor-cell engraftment, there was moderately more expansion of the OT-I pool than of the H-Y pool (**Fig. 7b**). The addition of simultaneous infection with *L. monocytogenes* Δ actA enhanced expansion of the OT-I population, as anticipated on the basis of published studies^{38,49}, but did not increase the population expansion of H-Y T cells and in fact caused a slight reduction in cell numbers (**Fig. 7a**). Accordingly, the addition of simultaneous infection with *L. monocytogenes* Δ actA greatly increased the difference between the H-Y population and OT-I population in terms of their size (**Fig. 7b**). We noted similar effects by the addition of infection with LCMV (**Fig. 7c,d**), and preliminary studies with coadministration of oligonucleotides containing the dinucleotide CpG (a Toll-like receptor 9 agonist), yielded comparable results (**Supplementary Fig. 6d**). These data suggested that while the CD5^{hi} OT-I clone responded to proinflammatory signals with enhanced expansion, this pathway was not operative in CD5^{lo} H-Y CD8⁺ T cells. The proinflammatory cytokines IL-12 and type I interferon act as a ‘third signals’ to promote CD8⁺ T cell responses^{46,47}, but preliminary *in vitro* experiments did not suggest differences in the responses of H-Y T cells versus OT-I T cells to those cytokines (data not shown), which indicated a more complex basis for the altered response. Nevertheless, our data suggested qualitative differences in the responses of CD5^{hi} CD8⁺ T cells versus those of CD5^{lo} CD8⁺ T cells when foreign-antigen stimulation was delivered in the context of innate immune cues *in vivo*.

DISCUSSION

Our data showed that naive CD8⁺ T cells with heightened recognition of self peptide-MHC ligands displayed enhanced reactivity toward foreign peptide-MHC antigens. We confirmed and extended the utility of CD5 expression as a measure of the strength of encounter with self ligand, showing that CD5^{hi} cells exhibited increased expression of the *Nur77*^{GFP} reporter (a surrogate of TCR signaling) and changes in gene expression indicative of enhanced response sensitivity. Comparison of the *in vivo* response to foreign antigen revealed multiple steps at which the CD5^{hi} population of naive CD8⁺ T cells manifested an advantage over their CD5^{lo} counterparts: their initial activation and response rates were more efficient, their clonal burst size was greater, and their sensitivity to inflammatory cues was enhanced. On the other hand, we did not observe a consistent difference in the capacity of polyclonal CD5^{hi} cells or CD5^{hi} cells with transgenic TCR expression to bind to foreign peptide-MHC tetramers versus that of their CD5^{lo} counterparts, nor did models of transgenic TCR expression suggest a difference in sensitivity of the response to foreign peptide-MHC. Together our studies support a model in which the differences between CD5^{hi} naive CD8⁺ T cells and CD5^{lo} naive CD8⁺ T cells are established before encounter with foreign antigen and various properties of the CD5^{hi} population make their responses more efficient and competitive.

Our data differ from two published reports that used CD5 expression to characterize heterogeneity in the responses of naive CD4⁺ T cells. While one study found that CD5^{hi} cells had enhanced engagement of the TCR with foreign peptide–MHC ligands and superior responses to antigen *in vivo*⁹, another reported that CD5^{lo} and CD5^{hi} cells had similar engagement with pMHC ligands and that CD5^{lo} cells showed greater population expansion *in vivo* than that of their CD5^{hi} counterparts^{10,11}. Although we observed some skewing in the size of the population that bound foreign peptide–MHC tetramers in favor of the CD5^{hi} pool, this effect was modest, and average tetramer-binding intensity was similar for antigen-specific CD5^{lo} cells and CD5^{hi} cells. Hence, our data and published data^{10,11} challenge the conceptually complex model that the structural ability to bind foreign peptide–MHC ligands is dictated by the sensitivity of T cells to self peptide–MHC. These discrepancies may reflect distinct properties of CD4⁺ T cells and CD8⁺ T cells⁹, although this argument does not pertain to the divergent conclusions reached by studies of CD4⁺ T cells^{9,11}. In any case, our findings reinforce the concept that, at least for naive CD8⁺ T cells, the distinct responses of the CD5^{hi} and CD5^{lo} populations probably reflect preexisting, intrinsic properties of the cells rather than arising from differences in perception of foreign antigen.

In contrast to our findings and other published results⁹, some reports have found that CD5^{lo} populations expand more effectively than do CD5^{hi} populations, despite having similar properties for the recognition of foreign ligands^{10,11}. Notably, published studies have argued that CD5^{hi} naive CD4⁺ T cells exhibit a strong response to stimulation via the TCR, but this leads to increased susceptibility to activation-driven cell death¹¹. Our data suggested that optimal population expansion of activated CD5^{hi} naive CD8⁺ T cells was dependent on CD25 expression, and enhanced sensitivity to IL-2 (through improved signaling via its receptor CD122) has been reported in studies of the homeostasis of CD5^{hi} naive CD8⁺ T cells²⁴. Enhanced sensitivity to IL-2 might be a boon to responding CD5^{hi} CD8⁺ T cells yet may be detrimental to CD5^{hi} CD4⁺ T cells (at least in some situations) by making them more vulnerable to induced cell death. We note that the range of CD5 expression (and associated basal TCR signaling) is greater in naive CD4⁺ T cells than in naive CD8⁺ T cells^{9–11}, which is perhaps indicative of distinct functional thresholds in these subsets.

Our studies build on considerable work suggesting that CD5 levels correlate with engagement of the TCR by self peptide–MHC^{9–11,18–21}. Our work has defined the properties of the CD5^{hi} population before antigen encounter, as well as the mechanisms by which these cells outcompete other naive CD8⁺ T cell populations during an active immune response. It is unclear whether CD5 itself contributes to the distinct functions of CD5^{hi} cells and CD5^{lo} cells; studies of *Cd5*^{-/-} mice do not support that concept^{9,11}, although this does not negate the value of CD5 expression as a marker. As we have shown here, the CD5^{hi} population differed from the CD5^{lo} population in the expression of several genes. However, even within the CD5^{hi} pool there was heterogeneity in the expression of T-bet and CXCR3 and induced expression of XCL1; hence, there may be other features of CD5^{hi} cells that better correlate with their improved functional prowess. We found a modest but significant advantage of CXCR3^{hi} CD5^{hi} populations over CXCR3^{lo} CD5^{hi} populations, which suggested that CXCR3 expression may be a core feature of the optimal reactivity of CD5^{hi} naive CD8⁺ T cells to foreign antigen.

Together these findings suggest that naive CD8⁺ T cells with the greatest self-reactivity are the cells most efficiently recruited into the foreign peptide–MHC–specific response. Since sensitivity to TCR signals may change following the activation of naive T cells, it is possible that progeny of some CD5^{hi} clones could exhibit overt self-reactivity

following activation, with relevance for the induction of autoimmune disease following the response to infection. At the same time, our findings leave open the question of why the CD5^{lo} pool is maintained in the naive CD8⁺ T cell repertoire. CD5^{lo} cells are relatively resistant to IL-7 deprivation²⁶, which indicates it possible that these cells are efficiently maintained during the competition of naive T cells for homeostatic cytokines. Alternatively, CD5^{lo} naive CD8⁺ T cells may show superior responses to pathogens in certain situations; as shown for naive CD4⁺ T cells, heightened initial reactivity may accompany increased sensitivity to cell death^{10,11}. Whether some immune responses favor the CD5^{lo} population of naive CD8⁺ T cells awaits further investigation.

METHODS

Methods and any associated references are available in the [online version of the paper](#).

Accession codes. GEO: microarray data, [GSE62142](#).

Note: Any Supplementary Information and Source Data files are available in the online version of the paper.

ACKNOWLEDGMENTS

We thank D. Masopust (University of Minnesota) for *Il15*^{-/-} mice, P14 mice and LCMV Armstrong strain; L. Cauley (University of Connecticut) for F5 mice deficient in recombination-activating gene 1; J. Zhu (National Institute of Allergy and Infectious Diseases) for T-bet–ZsGreen reporter mice; J. Harty (University of Iowa) for *L. monocytogenes* strain Δ actA (DP-L1942) and OVA-expressing *L. monocytogenes* Δ actA; R. Kedl (National Jewish Medical Research Center) for LM-B8R (virulent and Δ actA); M. Prlic and M. Bevan (University of Washington) and J. Harty (University of Iowa) for Flt3L-expressing B16 cells; R. Kroccek (Robert Koch-Institute) for the conjugated monoclonal antibody MTAC-2; the University of Minnesota Flow Core personnel for flow-cytometry support and cell sorting; M. Jenkins and M. Mescher for critical review of the manuscript; G. Sritesky for insight on the analysis of *Nur77* mice; J. Ding and S. Peery for technical assistance with mice; and members of the Jamequist laboratory for discussions. Supported by the US National Institutes of Health (R37 AI-38903 to S.C.J.; P30 CA77598, with the Biostatistics and Bioinformatics Core shared resource of the Masonic Cancer Center, University of Minnesota; UL1TR000114 from the National Center for Advancing Translational Sciences) and the Irvington Institute Fellowship Program of the Cancer Research Institute (R.B.F.). The content is solely the responsibility of the authors and does not necessarily represent the official views of the US National Institutes of Health.

AUTHOR CONTRIBUTIONS

R.B.F. and S.C.J. designed the experimental approaches; R.B.F. and S.E.H. conducted experiments; Y.X. and K.A.H. provided mouse strains and bone marrow chimeras; J.A.B. and A.W.G. analyzed gene-expression data; and R.B.F. and S.C.J. wrote and edited the manuscript.

COMPETING FINANCIAL INTERESTS

The authors declare no competing financial interests.

Reprints and permissions information is available online at <http://www.nature.com/reprints/index.html>.

- Zehn, D., Lee, S.Y. & Bevan, M.J. Complete but curtailed T-cell response to very low-affinity antigen. *Nature* **458**, 211–214 (2009).
- Tube, N.J. *et al.* Single naive CD4⁺ T cells from a diverse repertoire produce different effector cell types during infection. *Cell* **153**, 785–796 (2013).
- Fazilleau, N., McHeyzer-Williams, L.J., Rosen, H. & McHeyzer-Williams, M.G. The function of follicular helper T cells is regulated by the strength of T cell antigen receptor binding. *Nat. Immunol.* **10**, 375–384 (2009).
- Plumlee, C.R., Sheridan, B.S., Cicek, B.B. & Lefrançois, L. Environmental cues dictate the fate of individual CD8⁺ T cells responding to infection. *Immunity* **39**, 347–356 (2013).
- Dorfman, J.R., Stefanova, I., Yasutomo, K. & Germain, R.N. CD4⁺ T cell survival is not directly linked to self-MHC-induced TCR signaling. *Nat. Immunol.* **1**, 329–335 (2000).
- Stefanová, I., Dorfman, J.R. & Germain, R.N. Self-recognition promotes the foreign antigen sensitivity of naive T lymphocytes. *Nature* **420**, 429–434 (2002).

7. Bhandoola, A. *et al.* Peripheral expression of self-MHC-II influences the reactivity and self-tolerance of mature CD4⁺ T cells: evidence from a lymphopenic T cell model. *Immunity* **17**, 425–436 (2002).
8. Hochweller, K. *et al.* Dendritic cells control T cell tonic signaling required for responsiveness to foreign antigen. *Proc. Natl. Acad. Sci. USA* **107**, 5931–5936 (2010).
9. Mandl, J.N., Monteiro, J.P., Vrsekoop, N. & Germain, R.N. T cell-positive selection uses self-ligand binding strength to optimize repertoire recognition of foreign antigens. *Immunity* **38**, 263–274 (2013).
10. Weber, K.S. *et al.* Distinct CD4⁺ helper T cells involved in primary and secondary responses to infection. *Proc. Natl. Acad. Sci. USA* **109**, 9511–9516 (2012).
11. Persaud, S.P., Parker, C.R., Lo, W.L., Weber, K.S. & Allen, P.M. Intrinsic CD4 T cell sensitivity and response to a pathogen are set and sustained by avidity for thymic and peripheral complexes of self peptide and MHC. *Nat. Immunol.* **15**, 266–274 (2014).
12. Starr, T.K., Jameson, S.C. & Hogquist, K.A. Positive and negative selection of T cells. *Annu. Rev. Immunol.* **21**, 139–176 (2003).
13. Tanchot, C., Lemonnier, F.A., Perarnau, B., Freitas, A.A. & Rocha, B. Differential requirements for survival and proliferation of CD8 naive or memory T cells. *Science* **276**, 2057–2062 (1997).
14. Takada, K. & Jameson, S.C. Self-class I MHC molecules support survival of naive CD8 T cells, but depress their functional sensitivity through regulation of CD8 expression levels. *J. Exp. Med.* **206**, 2253–2269 (2009).
15. Takada, K. & Jameson, S.C. Naive T cell homeostasis: from awareness of space to a sense of place. *Nat. Rev. Immunol.* **9**, 823–832 (2009).
16. Sprent, J. & Surh, C.D. Normal T cell homeostasis: the conversion of naive cells into memory-phenotype cells. *Nat. Immunol.* **12**, 478–484 (2011).
17. Tarakhovskiy, A. *et al.* A role for CD5 in TCR-mediated signal transduction and thymocyte selection. *Science* **269**, 535–537 (1995).
18. Azzam, H.S. *et al.* CD5 expression is developmentally regulated by T cell receptor (TCR) signals and TCR avidity. *J. Exp. Med.* **188**, 2301–2311 (1998).
19. Wong, P., Barton, G.M., Forbush, K.A. & Rudensky, A.Y. Dynamic tuning of T cell reactivity by self-peptide-major histocompatibility complex ligands. *J. Exp. Med.* **193**, 1179–1187 (2001).
20. Smith, K. *et al.* Sensory adaptation in naive peripheral CD4 T cells. *J. Exp. Med.* **194**, 1253–1261 (2001).
21. Seddon, B. & Zamoyska, R. TCR signals mediated by Src family kinases are essential for the survival of naive T cells. *J. Immunol.* **169**, 2997–3005 (2002).
22. Kieper, W.C., Burghardt, J.T. & Surh, C.D. A role for TCR affinity in regulating naive T cell homeostasis. *J. Immunol.* **172**, 40–44 (2004).
23. Ge, Q., Bai, A., Jones, B., Eisen, H.N. & Chen, J. Competition for self-peptide-MHC complexes and cytokines between naive and memory CD8⁺ T cells expressing the same or different T cell receptors. *Proc. Natl. Acad. Sci. USA* **101**, 3041–3046 (2004).
24. Cho, J.H., Kim, H.O., Surh, C.D. & Sprent, J. T cell receptor-dependent regulation of lipid rafts controls naive CD8⁺ T cell homeostasis. *Immunity* **32**, 214–226 (2010).
25. Johnson, L.D. & Jameson, S.C. Self-specific CD8⁺ T cells maintain a semi-naive state following lymphopenia-induced proliferation. *J. Immunol.* **184**, 5604–5611 (2010).
26. Palmer, M.J., Mahajan, V.S., Chen, J., Irvine, D.J. & Lauffenburger, D.A. Signaling thresholds govern heterogeneity in IL-7-receptor-mediated responses of naive CD8⁺ T cells. *Immunol. Cell Biol.* **89**, 581–594 (2011).
27. Park, J.H. *et al.* 'Coreceptor tuning': cytokine signals transcriptionally tailor CD8 coreceptor expression to the self-specificity of the TCR. *Nat. Immunol.* **8**, 1049–1059 (2007).
28. Kaech, S.M. & Cui, W. Transcriptional control of effector and memory CD8⁺ T cell differentiation. *Nat. Rev. Immunol.* **12**, 749–761 (2012).
29. Judge, A.D., Zhang, X., Fujii, H., Surh, C.D. & Sprent, J. Interleukin 15 controls both proliferation and survival of a subset of memory-phenotype CD8⁺ T cells. *J. Exp. Med.* **196**, 935–946 (2002).
30. Moran, A.E. *et al.* T cell receptor signal strength in Treg and iNKT cell development demonstrated by a novel fluorescent reporter mouse. *J. Exp. Med.* **208**, 1279–1289 (2011).
31. Chang, J.T. *et al.* Asymmetric proteasome segregation as a mechanism for unequal partitioning of the transcription factor T-bet during T lymphocyte division. *Immunity* **34**, 492–504 (2011).
32. Miller, A.T., Wilcox, H.M., Lai, Z. & Berg, L.J. Signaling through Itk promotes T helper 2 differentiation via negative regulation of T-bet. *Immunity* **21**, 67–80 (2004).
33. Dorner, B.G. *et al.* Selective expression of the chemokine receptor XCR1 on cross-presenting dendritic cells determines cooperation with CD8⁺ T cells. *Immunity* **31**, 823–833 (2009).
34. Best, J.A. *et al.* Transcriptional insights into the CD8⁺ T cell response to infection and memory T cell formation. *Nat. Immunol.* **14**, 404–412 (2013).
35. Haluszczak, C. *et al.* The antigen-specific CD8⁺ T cell repertoire in unimmunized mice includes memory phenotype cells bearing markers of homeostatic expansion. *J. Exp. Med.* **206**, 435–448 (2009).
36. Sung, J.H. *et al.* Chemokine guidance of central memory T cells is critical for antiviral recall responses in lymph nodes. *Cell* **150**, 1249–1263 (2012).
37. Kastenmüller, W. *et al.* Peripheral prepositioning and local CXCL9 chemokine-mediated guidance orchestrate rapid memory CD8⁺ T cell responses in the lymph node. *Immunity* **38**, 502–513 (2013).
38. Starbeck-Miller, G.R., Xue, H.H. & Harty, J.T. IL-12 and type I interferon prolong the division of activated CD8 T cells by maintaining high-affinity IL-2 signaling in vivo. *J. Exp. Med.* **211**, 105–120 (2014).
39. Malek, T.R. & Castro, I. Interleukin-2 receptor signaling: at the interface between tolerance and immunity. *Immunity* **33**, 153–165 (2010).
40. Buchholz, V.R. *et al.* Disparate individual fates compose robust CD8⁺ T cell immunity. *Science* **340**, 630–635 (2013).
41. Gerlach, C. *et al.* Heterogeneous differentiation patterns of individual CD8⁺ T cells. *Science* **340**, 635–639 (2013).
42. van Heijst, J.W. *et al.* Recruitment of antigen-specific CD8⁺ T cells in response to infection is markedly efficient. *Science* **325**, 1265–1269 (2009).
43. Daniels, M.A. & Jameson, S.C. Critical role for CD8 in T cell receptor binding and activation by peptide/major histocompatibility complex multimers. *J. Exp. Med.* **191**, 335–346 (2000).
44. Haring, J.S., Badovinac, V.P. & Harty, J.T. Inflaming the CD8⁺ T cell response. *Immunity* **25**, 19–29 (2006).
45. Cui, W. & Kaech, S.M. Generation of effector CD8⁺ T cells and their conversion to memory T cells. *Immunol. Rev.* **236**, 151–166 (2010).
46. Badovinac, V.P., Messingham, K.A., Jabbari, A., Haring, J.S. & Harty, J.T. Accelerated CD8⁺ T-cell memory and prime-boost response after dendritic-cell vaccination. *Nat. Med.* **11**, 748–756 (2005).
47. Curtsinger, J.M. & Mescher, M.F. Inflammatory cytokines as a third signal for T cell activation. *Curr. Opin. Immunol.* **22**, 333–340 (2010).
48. Maile, R. *et al.* Peripheral "CD8 tuning" dynamically modulates the size and responsiveness of an antigen-specific T cell pool *in vivo*. *J. Immunol.* **174**, 619–627 (2005).
49. Pham, N.L., Badovinac, V.P. & Harty, J.T. A default pathway of memory CD8 T cell differentiation after dendritic cell immunization is deflected by encounter with inflammatory cytokines during antigen-driven proliferation. *J. Immunol.* **183**, 2337–2348 (2009).
50. Zhu, J. *et al.* The transcription factor T-bet is induced by multiple pathways and prevents an endogenous Th2 cell program during Th1 cell responses. *Immunity* **37**, 660–673 (2012).

ONLINE METHODS

Mice. We purchased 6- to 12-week-old female C57BL/6 and B6.SJL mice from the National Cancer Institute. For recipients of adoptively transferred cells, we used F₁ CD45.1/2 females generated from C57BL/6J mice (Jackson Laboratories) crossed with B6.SJL mice (National Cancer Institute). *I15*^{-/-} mice and P14 mice (with transgenic expression of a TCR specific for LCMV gp33)⁵¹ were gifts from D. Masopust. P14 and OT-I mice⁵² were maintained on a C57BL/6N and B6.PL (Thy-1.1⁺) backgrounds. H-Y mice were maintained on a background deficient in recombination-activating gene 2 (*Rag2*^{-/-}) (apart from initial cell surface phenotype studies, in which cells from female *Rag2*^{+/+} H-Y mice were analyzed with monoclonal antibody T3.70 to identify H-Y-specific CD8⁺ T cells). F5 mice deficient in recombination-activating gene 1 (*Rag1*^{-/-} mice) were a gift from L. Cauley, and *Cd25*^{-/-} mice were obtained from Jackson Labs. The *Nur77*^{GFP} transgenic reporter mice have been described³⁰ and were maintained on a C57BL/6N background. T-bet-ZsGreen reporter mice⁵⁰ were initially obtained from J. Zhu and were maintained on the C57BL/6N background. All mice were maintained in specific pathogen-free conditions, and all mouse protocols were approved by the University of Minnesota Institutional Animal Care and Use Committee. No samples or animals were excluded from the analysis. The investigators were not blinded to group allocations or assessment.

Bacterial and viral infection. The attenuated *L. monocytogenes* strain Δ actA (DP-L1942)⁵³ and OVA-expressing *L. monocytogenes* Δ actA were provided by J. Harty, and LM-B8R (both virulent and Δ actA), which contains both the H-2K^b-restricted CD8⁺ epitopes B8R (amino acids 20–27) and OVA (amino acids 257–264), was a gift from R. Kedl. LCMV, Armstrong strain, was a gift from D. Masopust. *L. monocytogenes* was grown in tryptic soy broth containing 50 μ g/ml streptomycin to an absorbance of ~0.1 at 600 nm. For primary infection with attenuated LM-B8R, 3 \times 10⁶ colony-forming units were injected intravenously into mice. For secondary infection with virulent LM-B8R, mice were given intravenous injection of 1 \times 10⁶ colony-forming units. In experiments in which wild-type *L. monocytogenes* Δ actA was used to induce inflammation, 3 \times 10⁶ to 6 \times 10⁶ colony-forming units of bacteria were mixed with peptide-pulsed DCs and the mixture was injected intravenously into mice. For infection with LCMV, mice were given intraperitoneal injection of 2 \times 10⁵ plaque-forming units.

Immunization with DCs. Splenic DCs were prepared as described⁴⁹. To generate splenic DCs, mice were given subcutaneous injection of 5 \times 10⁶ B16 mouse melanoma cells expressing the cytokine Flt3L (provided by M. Prlic and M. Bevan, via J. Harty). When tumors were palpable (5 mm \times 5 mm), mice were given intravenous injection of 2 μ g lipopolysaccharide to mature the DCs, and spleens were collected ~16 h later. Following digestion for 20 min at 37 °C with collagenase D, red blood cells were lysed, and splenocytes were resuspended in medium composed of two parts complete RPMI medium (RPMI-1640 medium containing 10% fetal calf serum, 5 mM HEPES, 50 U/ml penicillin (sodium salt), 50 μ g/ml streptomycin sulfate, 2 mM L-glutamine, 50 μ M 2-mercaptoethanol and 50 μ g/ml gentamycin sulfate) mixed with one part complete RPMI medium conditioned by Flt3L-expressing B16 cells, 50 ng/ml granulocyte-macrophage colony-stimulating factor and 2 μ M peptide. The C2A mutant of the Smcy peptide⁵⁴ was used for the stimulation of H-Y CD8⁺ T cells, while OVA peptide was used for the stimulation of OT-I cells. Splenocytes were pulsed for 2 h at 37 °C with peptide, then were thoroughly washed, and DCs were purified with Miltenyi CD11c microbeads. Mice were given intravenous injection of 1 \times 10⁶ DCs pulsed with each peptide along with coadministration of *L. monocytogenes*, LCMV or CpG.

Flow cytometry. Cells were stained with the following antibodies (all antibodies from eBioscience or BD Biosciences unless noted otherwise): anti-CD4 (RM4-5), anti-CD8 (53-6.7), anti-CD5 (53-7.3), anti-CD27 (LG.7F9), anti-CD44 (IM7), anti-CD45.1 (A20), anti-CD45.2 (104), anti-Thy-1.1 (HIS51 or OX-7), anti-Thy-1.2 (53-2.1), anti-CD62L (MEL-14), anti-CD69 (H1.2F3), anti-CD122 (TM-b1), anti-CD127 (A7R34), anti-TCR β (H57-597), anti-CXCR3 (CXCR3-173), anti-interferon- γ (XMG1.2), anti-MHC class II (M5/114.15.2) and anti-F4/80 (BM8). The B8R-H-2K^b and OVA-H-2K^b tetramers were generated as described⁴³. The mouse cytomegalovirus M57-H-2K^b, LCMV

gp33-H-2D^b, influenza virus NP68-H-2D^b and H-Y Smcy-H-2D^b tetramers were provided by the NIH Tetramer Facility. For intracellular staining of transcription factors, cells were fixed and permeabilized with Foxp3 Fixation and Permeabilization Buffers (eBioscience) and were stained with anti-T-bet (4B10) and anti-eomesodermin (Dan11mag) in Permeabilization Solution. Data were collected on an LSR II or Fortessa flow cytometer (BD Biosciences), and data were analyzed with FlowJo analysis software (TreeStar).

XCL1 expression assay. Peripheral lymphocytes were stained with monoclonal antibody to XCL1 (MTAC-2)⁵⁵ provided by R. Kroczek (Robert Koch-Institute, Berlin, Germany). For analysis of XCL1 production, bulk splenocytes were stimulated for 3–5 h at 37 °C with PMA (phorbol 12-myristate 13-acetate) and ionomycin in the presence of brefeldin A. Cells were stained for cell surface markers, then were fixed and permeabilized with BD Cytotfix/Cytoperm or eBiosciences Foxp3/transcription factor fixation/permeabilization solutions, before intracellular staining for XCL1.

Cell sorting and adoptive transfer. For adoptive-transfer experiments, spleens and lymph nodes from C57BL/6 (CD45.2⁺CD45.2⁺) mice and B6.SJL (CD45.1⁺CD45.1⁺) mice were digested with collagenase D (Roche) and underwent negative enrichment for CD8⁺ T cells with Miltenyi enrichment antibody 'cocktail' and beads. Cells were then stained with anti-CD8, anti-CD5 and anti-CD44 (antibodies identified above), and CD8⁺CD44^{lo} cells (i.e., samples from which CD44^{hi} cells were excluded) were sorted on the lower or upper 20% of CD5 expression with a FACSAria I (BD). In some studies, the CD5^{hi} CD44^{lo} population was further gated on the lower or upper 30% of CXCR3 expression before sorting. Approximately 1.25 \times 10⁶ to 1.5 \times 10⁶ cells of each of the congenically mismatched CD5^{lo} and CD5^{hi} cell populations were transferred together into CD45.1⁺CD45.2⁺ recipients that that infected with LM-B8R the next day. For recall experiments, CD5^{lo} and CD5^{hi} recipients that had been infected with B8R-expressing *L. monocytogenes* Δ actA >40 d previously were challenged with virulent LM-B8R. Various combinations of congenic backgrounds for donor and host mice were used in transfer studies.

In experiments in which we transferred single B8R-H-2K^b-specific CD8⁺ T cell clones, CD8⁺ T cells underwent negative enrichment from the spleens and lymph node cells of 4 to 8 congenically distinct donors through the use of different combinations of CD45.1 and CD45.2 as well as CD90.1 and CD90.2 (Supplementary Fig. 4) (antibodies identified above). Equal numbers of CD8⁺ T cells from each congenic donor group were mixed, stained with anti-CD8, anti-CD5 and anti-CD44 (antibodies identified above) and sorted as naive CD8⁺ T cells in the lower or upper 20% of CD5 expression. The appropriate number of CD5^{lo} and CD5^{hi} cells from each congenic group was then transferred into congenic recipients. Mice were infected 1–2 d after transfer with attenuated LM-B8R, and the response to B8R-H-2K^b was assessed 7 d later. Background staining for congenic markers was very low (one event or less; data not shown), and we set our limit of detection at three or more flow cytometry events in the antigen-specific population, which is equal to about five total B8R-H-2K^b-specific CD8⁺ T cells.

In adoptive-transfer experiments with CD8⁺ T cells with transgenic TCR expression, CD44^{lo} Thy-1.1⁺ OT-I cells (*Rag1*^{+/+} or *Rag1*^{-/-}) underwent enrichment by negative selection as described⁵⁶. *Rag2*^{-/-} H-Y CD8⁺ T cells from female mice, which are all CD44^{lo} cells, underwent negative enrichment with Miltenyi beads. Mixtures containing 1 \times 10³ cells of the OT-I population and 1 \times 10³ cells of the H-Y population were transferred intravenously into B6.SJL mice, and these recipients were immunized 1 d later. For analysis of the 'take', 2 \times 10⁵ cells from the same mixture of OT-I and H-Y cells was transferred into recipients, and cells from these mice were then analyzed by flow cytometry on the day of immunization. Similar 'take' ratios were observed for mice that received 1 \times 10³ OT-I and H-Y T cells that underwent enrichment by magnetic beads on the day of immunization (data not shown).

Enrichment with MHC class I tetramers. For analysis of antigen-specific precursors of CD8⁺ T cells or CD5^{lo} or CD5^{hi} donor responses following infection, enrichment by MHC class I tetramers was used as described³⁵. Spleens and lymph nodes (for analysis of precursors) or spleens only (for infection with *L. monocytogenes*) were digested with collagenase D. Cells were labeled with phycoerythrin- or allophycocyanin-conjugated tetramers and underwent

enrichment over magnetic columns with anti-phycoerythrin or anti-allophycocyanin magnetic beads (Miltenyi). A small portion of the enriched fraction was added to AccuCheck counting beads (Invitrogen) for accurate back-calculation of total numbers. Fractions enriched for tetramers were then stained with additional extracellular antibodies (identified above) and were fixed with paraformaldehyde before analysis by flow cytometry.

Mixed bone marrow chimeras. We generated mixed-bone marrow chimeras by obtained bone marrow from congenic strains, depleting the bone marrow of T cells and mixing the bone marrow from the different strains, and then injecting 5×10^6 to 10×10^6 cells into lethally irradiated (1,000 rads) host mice. For chimeras reconstituted with wild-type and *Cd25*^{-/-} bone marrow, roughly equal numbers of cells from wild-type (CD45.1⁺CD45.2⁺) mice and *Cd25*^{-/-} (CD45.2⁺) mice (6–8 weeks of age) were injected into wild-type (CD45.1⁺) hosts. For OT-I chimeras, OT-I (RAG⁺) bone marrow with disparate allelic expression of the alloantigen Thy-1 was injected into congenically distinct wild-type or β_2 -microglobulin-deficient recipients. Cells from chimeras were used >10 weeks after transplantation.

In vitro stimulation. For analysis of CD8⁺ T cell activation, 2×10^4 purified CD44^{lo} CD8⁺ cells with transgenic TCR expression were incubated at 37 °C with 1×10^6 to 2×10^6 splenic antigen-presenting cells in 96-well round-bottomed plates with titrated doses of cognate peptide: OT-I cells were incubated with OVA-H-2K^b (OVA amino acids 257–264: SIINFEKL), P14 cells were incubated with gp33-H-2D^b (gp amino acids 33–41: KAVYNFATC), F5 cells were incubated with NP366-H-2D^b (NP amino acids 366–374; ASNENMDAM), and H-Y cells were incubated with Smcy-H-2D^b (KCSRNRQYL) or C2A-H-2D^b (KASRNQYL). Cells were stimulated for 6 h and then stained for CD69 expression.

Assay of MHC class I stabilization in RMA-S cells. RMA-S cells were cultured at 30 °C with 5% CO₂ overnight in RPMI medium containing 10% FCS. In a 96-well round-bottomed plate, 1×10^5 RMA-S cells were incubated for 1 h with titrated doses of peptide and then the plate was moved to a 37 °C CO₂ incubator for 3 h. Stable surface MHC class I molecules on cells were then stained with antibody to H-2K^b (Y3) or H-2D^b (28.14.8) (both produced at the University of Minnesota).

Gene-transcription analysis. Naive CD44^{lo} CD8⁺ T cells from spleens and lymph nodes were sorted by flow cytometry as cells with the lower and upper

20% of CD5 expression as described above. For each sample, $\geq 1 \times 10^6$ cells were used for RNA extraction with an RNeasy microkit (Qiagen). RNA was used to generate biotinylated cRNA with a MessageAmpIII RNA Amplification kit according to the manufacturer's recommendations (Ambion). Samples were hybridized to Affymetrix murine 430 2.0 gene chips at the BioMedical Genomics Center (University of Minnesota) by standard procedures. RNA samples from three independent sorts were analyzed. Genespring software was used to generate gene-expression analysis for **Table 1**: data were normalized with the MAS5 algorithm and were filtered for present or absent 'calls' in at least one group and for a significant ($P < 0.05$) difference in expression of twofold or more. For enrichment analysis (**Table 2**), cluster genes expressed by either CD5^{hi} cells or CD5^{lo} cells were determined to be any genes with a change in expression of >0. Significance was determined by χ^2 , in which equal distribution was taken as the null hypothesis.

Statistics. Unless indicated otherwise in the figure legend(s), a two-tailed, unpaired Student's *t*-test was performed on log-transformed data with Prism (GraphPad Software). For multiple comparisons, one-way analysis of variance with Dunnett's multiple-comparison post-test was used. Sample sizes were chosen on the basis of previous experience and similar studies. In the clonal analysis in **Figure 4**, the data distribution was not normal or log-normal, and the nonparametric Mann-Whitney test was applied.

51. Pircher, H., Rohrer, U.H., Moskophidis, D., Zinkernagel, R.M. & Hengartner, H. Lower receptor avidity required for thymic clonal deletion than for effector T-cell function. *Nature* **351**, 482–485 (1991).
52. Hogquist, K.A. *et al.* T cell receptor antagonist peptides induce positive selection. *Cell* **76**, 17–27 (1994).
53. Brundage, R.A., Smith, G.A., Camilli, A., Theriot, J.A. & Portnoy, D.A. Expression and phosphorylation of the *Listeria monocytogenes* ActA protein in mammalian cells. *Proc. Natl. Acad. Sci. USA* **90**, 11890–11894 (1993).
54. Maile, R. *et al.* Antigen-specific modulation of an immune response by in vivo administration of soluble MHC class I tetramers. *J. Immunol.* **167**, 3708–3714 (2001).
55. Dorner, B.G. *et al.* MIP-1 α , MIP-1 β , RANTES, and ATAC/lymphotactin function together with IFN- γ as type 1 cytokines. *Proc. Natl. Acad. Sci. USA* **99**, 6181–6186 (2002).
56. Kieper, W.C., Prlc, M., Schmidt, C.S., Mescher, M.F. & Jameson, S.C. IL-12 enhances CD8 T cell homeostatic expansion. *J. Immunol.* **166**, 5515–5521 (2001).